Analysis of Model Implied Volatility for Jump Diffusion Models: Empirical Evidence from the Nordpool Market

Nikos K Nomikos* and **Orestes A Soldatos****

ABSTRACT

In this paper we examine the importance of mean reversion and spikes in the stochastic behaviour of the underlying asset when pricing options on power. We propose a model that is flexible in its formulation and captures the stylized features of power prices in a parsimonious way. The main feature of the model is that it incorporates two different speeds of mean reversion to capture the differences in price behaviour between normal and spiky periods. We derive semi-closed form solutions for European option prices using transform analysis and then examine the properties of the implied volatilities that the model generates. We find that the presence of jumps generates prominent volatility skews which depend on the sign of the mean jump size. We also show that mean reversion reduces the volatility smile as time to maturity increases. In addition, mean reversion induces volatility skews particularly for ITM options, even in the absence of jumps. Finally, jump size volatility and jump intensity mainly affect the kurtosis and thus the curvature of the smile with the former having a more important role in making the volatility smile more pronounced and thus increasing the kurtosis of the underlying price distribution.

Keywords: Affine Jump Diffusion Model, Implied Volatility, Volatility Skew, Electricity Derivatives, Risk Management
JEL Classification: G13, G12 and G33

Acknowledgements: We are grateful to Derek Bunn and John Hatgioannides for suggesting useful improvements.

* Corresponding Author: Faculty of Finance, Cass Business School, London EC1Y 8TZ, UK.
email: n.nomikos@city.ac.uk; tel: +44 207040 0104: fax: +44 207040 8681
** Research, Total Gas & Power Ltd, London E14 5BF, UK.
email: orestes.soldatos@total.com; tel: +44 207718 6890; fax: +44 207718 6559

1 Introduction

Over the last 10 years radical changes have taken place in the structure of electricity markets around the world. Following the deregulation of power markets, prices are now determined under the fundamental rule of supply and demand and the resulting price volatility has increased the need for risk management using derivative contracts such as futures and options. It is important therefore for market participants to use option pricing models that can price fairly the most significant risks that exist in the market. However, due to the unique features of power markets, the traditional approaches for the pricing of derivatives that are used in other financial and commodity markets are not applicable to electricity. For instance, electricity is a non-storable commodity and a non-tradable asset which implies that arbitrage across time and space is limited. In addition, electricity prices exhibit extreme movements and volatility over short periods of time and are characterised by spikes which occur due to short-term supply shocks. Given these features of power prices, the assumption used in the Black-Scholes-Merton (BSM) model (Black and Scholes, 1973 and Merton, 1973) that the underlying asset follows a log-normal random walk, may not be appropriate.

The issue of modelling power prices has been investigated extensively in the literature. For instance, Lucia and Schwartz (2002) use a mean reverting process, as in Vasicek (1977), and a two-factor model, along the lines of Schwartz and Smith (2000), to model power prices in Nordpool. Villaplana (2003) introduces a two-factor jump-diffusion model and shows the significance of jumps in explaining the seasonal forward premium in the market. Bessembinder and Lemmon (2001) and Longstaff and Wang (2002) show that the sign and size of the forward premium is related to economic risks and the willingness of market participants to bear those risks. Geman and Roncoroni (2006) introduce a marked-point process calibrated to capture the trajectoral and statistical features of power prices. Weron (2008) models Nord Pool prices using a jump diffusion model and Nomikos and Soldatos (2008) apply a seasonal affine jump diffusion model with regime switching in the long-run equilibrium level to model spot and forward prices in the same market.

In this paper we investigate empirically the performance of option pricing models that take into account the existence of mean-reversion and spikes in the stochastic behaviour of power prices. In particular, we examine the performance of a spike mean-reverting model that

incorporates two different speeds of mean reversion - one for the diffusive part of the model and another one for the spikes - in order to capture the spiky behaviour of jumps and the slower mean reversion of the diffusive part of the model. Spikes are short-lived price movements of the spot market that do not spill-over to the forward market and, as such, they mean-revert at a much faster speed than ordinary shocks in the market. The proposed model is flexible in its formulation and encompasses the stylised features of many of the deregulated electricity markets around the world, as these have been identified in the literature. Therefore, although the model is calibrated to the Nordpool market, our results apply in general to other power markets as well.

The performance of the spike option pricing model is assessed empirically on the basis of the model implied volatilities that it generates; that is, the implied volatilities for which the option price from the BSM model matches the price from the proposed spike model. Model implied volatilities provide a very useful framework for assessing the performance of option pricing models as they illustrate the volatility shape and term structure that a model can theoretically capture in the market. The use of model implied volatilities is also justified by the fact that the market for exchange traded options in power is not liquid and thus, we cannot rely on traded option prices to assess the fit of the model in the market. The analysis of model implied volatilities has received little attention in the options pricing literature for the power markets, although the same methodology has been applied for instance in the equity options markets by Branger (2004) who compares model implied volatilities generated using Merton's (1976) jump diffusion and Heston's (1993) stochastic volatility models**.** In fact, the proposed methodology can be applied to markets for which liquid option markets do not exist but, the pricing of options, for either over-the-counter trading or for real options applications, is important and thus, one wants to test the validity and properties of alternative option pricing models.

In the paper, we derive the theoretical moments of the risk-neutral distribution implied by the spike model, as these provide information regarding the skewness and kurtosis of the implied volatility surfaces, and then examine the properties of the implied volatility shape using as a benchmark the traditional Black-Scholes-Merton model. This way, we are able to investigate whether the proposed model can capture the volatility smiles and smirks that are anticipated in the market, and also identify the model parameters that play the most important role in terms of shaping the volatility structure across maturities and strikes. In order to calculate the

implied volatilities, we derive semi-closed form solutions for European options based on the spike model, using the transform analysis by Duffie et al (2000). Our results indicate that the volatility skew depends primarily on the size and sign of the spikes whereas, it is the jump size volatility - rather than the jump intensity - that plays more important role in making the volatility smile more pronounced and thus increasing the kurtosis of the price distribution. Furthermore, even in the absence of spikes, we find that implied volatilities exhibit skewness since mean reversion does not allow the underlying prices to reach very high or low price levels, thus reducing the probability of an out-of-the-money option ending in-the-money

The structure of this paper is as follows: the following section reviews the theory of option pricing and derives semi-closed form solutions for the spike model. In section 3 we derive the theoretical moments of the risk neutral distribution of the spike model. Section 4 presents the model implied volatilities generated by the model using different model parameters each time and providing intuitive explanations in terms of the moments of the underlying price distribution. Finally, Section 5 concludes the paper.

2 Options Pricing using the spike model

Modelling electricity prices presents a number of challenges for researchers for a number of reasons. Power prices tend to fluctuate around values determined by the marginal cost of generating electricity and the level of demand, in other words they have a tendency of *mean reversion* to an equilibrium price, which is a common feature of most commodity markets. Power prices also tend to change by the time of day, week or month and in response to cyclical fluctuations in demand, and thus contain a *seasonality* component. In addition, the *non-storability* of electricity means that inventories cannot be used to smooth-out temporal supply-demand imbalances which results in high volatility. This, coupled with supply-side shocks such as generating or transmission constraints and unexpected outages, cause temporary price "*spikes*" due to restrictions in the available capacity which may take from a few hours up to a few days to fix; in other words, electricity prices may jump to a new level of, say, ten times their mean, but they do not stay there for long as they quickly revert back to their mean level. Similarly, spikes may also occur due to the inelasticity of demand which, combined with the convex shape of the supply stack, means that a given increase in demand may result in a large increase in the equilibrium price. At this high level then, more generators

will enter the market to take advantage of the higher price thus forcing the price to revert back to its long-run mean. There is also another implication of the convex shape of the supply stack; at higher price levels the supply stack curve becomes steeper and steeper, hence price changes are bigger for a given change in demand, causing an asymmetry in the volatility. This is exactly the opposite from what is noticed in the equity markets, and is known as the *inverse leverage effect* (see e.g. Geman, 2005).

Therefore, electricity prices have the tendency to mean-revert to an equilibrium level which also implies a decreasing volatility term structure as time to maturity increases. This phenomenon, known as the Samuelson effect (1965), is due to the fact that for non-storable commodities, such as electricity, any new information in the market will have a more prominent effect on derivative prices that are closer to maturity. Electricity prices also exhibit very high volatility, where spikes play a major role. In general, when spikes occur they do not spill over to the forward market, since they are short lived. (Geman, 2005) On the other hand, the existence of spikes induces excess skewness and kurtosis to the distribution of spot electricity prices, and this also has a direct impact on option prices, especially for out-of-the-money (OTM) call options which now have higher probability of ending in-the-money (ITM), compared to the BSM model. This is also what causes the implied volatility from market prices in the BSM model not to be constant across strike prices but to have a smile or smirk shape as it will be shown in the next section.

These properties of power prices can be captured by the seasonal spike mean-reverting model where the spot price, P_t, is modelled as the sum of a deterministic seasonal component, *f(t)*, and the exponential sum of a stochastic component, X_t , which follows a stationary (as in Vasicek, 1977) process reverting to an equilibrium value, and a spike factor, *Y*, as follows:

$$\begin{aligned} P_t &= f(t) + \exp(X_t + Y_t) \\ dX_t &= \left(k_1\left(\varepsilon - X_t\right) - \lambda_X\right)dt + \sigma_X dW_X^* \\ dY_t &= -k_2 Y_t dt + J(\mu_J, \sigma_J^2)dq(l) \end{aligned} \qquad (1)$$

In equation (1), k_1 represents the speed at which *X* reverts to its mean-equilibrium value under the risk-neutral probability measure, $\tilde{\varepsilon} = \varepsilon - \lambda_X / k_1$, after a shock has occurred; dW_X^*

represents the increment of a Brownian motion that causes the random shocks in the short-term factor, X, and is scaled up by the volatility factor σ_x; k_2 is the speed of mean reversion of the spike factor, Y, and the arrival of shocks is modelled via a compound Poisson process with intensity l. The distribution of the jump size is assumed to be Normal with mean μ_J, and standard deviation σ_J. Since the spike shock is expected to have a much shorter life than a normal shock, k_2 should be larger than k_1; finally, λ_X is the market price of risk that is asked in order for participants to trade derivatives in the power market.

It has been shown empirically that the proposed model provides very good fit to power prices in terms of capturing their distributional and trajectoral properties. For instance, Nomikos and Soldatos (2008) compare a number of models in terms of their fit to spot and forward prices in Nordpool, and find that the spike model of equation (1) provides superior fit compared to ordinary mean reversion and jump diffusion models. The major feature of the spike model is that it incorporates two different speeds of mean reversion: one for the diffusive part of the model and one for the spikes, with the latter being much higher in order to capture the fast decay of jumps in the market. The justification for that is that spikes are short-lived price movements of the spot market that do not spill-over to the forward market; in order to ensure this, it is necessary to have a faster speed of mean reversion for the spikes. The importance of incorporating spike mean reversion in modelling power prices has been emphasised in a number of studies such as Geman and Roncoroni (2006), Weron (2008) and Huisman (2009). The advantage of the spike model proposed here is that we can use transform analysis (Duffie et al, 2000) to derive semi-closed form solutions for option prices.

From the modelling point of view, the existence of spikes implies that the use of a simple mean-reversion model is not appropriate since it cannot capture adequately the dynamics in the spot market. On the other hand, modelling prices using an ordinary jump-diffusion model (as in Clewlow and Strickland**,** 2000) will result in the jump component being transferred to the forward prices as well, particularly if the speed of mean reversion in the market is not fast enough. Also, such a model will not be able to capture the spiky nature of the jump, especially in cases where shocks in the market die out at a slower rate. Therefore, the proposed model accounts for the difference in the speed of mean-reversion when normal shocks occur in the market, due to say variations in weather conditions or market behaviour, and when jump shocks occur due to an outage or a major generator coming out of the system for a few hours or days. Overall, the model is general in its formulation and captures the stylized features of

power markets - i.e. slow mean reversion for diffusive risk, spikes that mean revert at a very fast rate, volatility term structure and seasonality - in a parsimonious way. Despite the attractive features of this model and its empirical application to spot and forward markets, the issue of options pricing in the power markets using the spike model has received little attention in the literature.

In the BSM model, the risk neutral density is lognormal and the expectation of the normalised option payoff can easily be calculated. In more sophisticated models, such as the mean-reverting jump diffusion model of Clewlow and Strickland (2000), there is no closed-form solution for the risk-neutral density. One can use the Transform Analysis by Duffie et al (2000) (see Appendix A) and implement the Fourier inversion theorem where numerical integration of the imaginary part of complex function is performed. [1] This type of solution is semi-closed since numerical integration has to be performed to calculate the density function. [2] To illustrate how transform analysis can be used to derive semi-closed form solutions for European option prices, as it is done by Duffie et al (2000), let us start by defining $G_{a,b}(y;\mathbf{X}_T)$ as the price of a security that pays $e^{a\boldsymbol{X}_T}$ at maturity when $b\boldsymbol{X}_T \le y$, where $\boldsymbol{X}_T$ is a vector of the state variables that describe the price process and in our case $\boldsymbol{X}_T = [X_T, Y_T]$. Also note that the price of a European call can be written as follows:

$$\begin{aligned} Call &= E^*\left[e^{-rT}\left(P_T - K\right)^+ / \mathcal{F}_0\right] = E^*\left[e^{-rT}\left(e^{1'\boldsymbol{X}_T} - DK\right)^+ / \mathcal{F}_0\right] \\ &= E^*\left[e^{-rT}e^{1'\boldsymbol{X}_T}1_{1'\boldsymbol{X}_T \ge \ln(DK)} / \mathcal{F}_0\right] - DK\ E^*\left[e^{-rT}1_{1'\boldsymbol{X}_T \ge \ln(DK)} / \mathcal{F}_0\right] \\ &= G_{1',-1'}\left(-\ln(DK); \boldsymbol{X}_T, T, \chi\right) - DK\ G_{0',-1'}\left(-\ln(DK); \boldsymbol{X}_T, T, \chi\right) \end{aligned} \qquad (2)$$

where: E^* denotes the expectation under the equivalent martingale measure; χ captures both the distribution of the vector prices $\boldsymbol{X}$ as well as the effects of discounting and determines the transform function in DPS (2000); 1´ and 0´ denote *2x1* transpose vectors of ones and zeros, respectively, and, *DK = K - f(T)* denotes the de-seasonalised strike price [3]. Equation (2)

[1] Transform functions, like Fourier or Laplace, are transformations made to a function in order to have an analytical treatment to a solution (e.g. to find a closed-form solution in options pricing). For applications of Fourier transforms in options pricing see Cerny (2009).

[2] Note however that even in the BSM model, as in any other model for which a closed-form solution for option prices exists, the calculation of the risk-neutral density function also involves numerical integration of the area under the normal distribution, which can nevertheless be easily calculated using statistical software or tables.

[3] The reason we use the de-seasonalised strike price follows from the fact that the seasonality component is the deterministic part of the spot and can thus be subtracted directly from the strike price. Thus, in a model where

suggests that the call option payoff is ITM when $X_T + Y_T > \ln(DK)$ or, alternatively, $-X_T - Y_T < -\ln(DK)$. Also, denote $\boldsymbol{v} = [v, v]$ the variable defining the Fourier Transform then, Duffie et al (2000) show that:

$$\begin{aligned} G_{1',-1'}\left(-\ln(DK); \boldsymbol{X}, T, \chi\right) &= \psi^{\chi}\left(1'\right) - \frac{1}{\pi}\int_0^{\infty} \frac{\mathrm{Im}\left[\psi^{\chi}\left(1' - i\boldsymbol{v}, \boldsymbol{X}, 0, T\right) e^{i\ln(DK)v}\right]}{\boldsymbol{v}} dv \\ &= \frac{e^{-rT} F\left(0, T, \boldsymbol{X}\right)}{2} - \frac{1}{\pi}\int_0^{\infty} \frac{\mathrm{Im}\left[\psi^{\chi}\left(1' - i\boldsymbol{v}, \boldsymbol{X}, 0, T\right) e^{i\ln(DK)v}\right]}{\boldsymbol{v}} dv \end{aligned} \tag{3}$$

$$\begin{aligned} G_{0',-1'}\left(-\ln(DK); \boldsymbol{X}, T, \chi\right) &= \frac{\psi^{\chi}\left(0'\right)}{2} - \frac{1}{\pi}\int_0^{\infty} \frac{\mathrm{Im}\left[\psi^{\chi}\left(-i\boldsymbol{v}, \boldsymbol{X}, 0, T\right) e^{i\ln(DK)v}\right]}{\boldsymbol{v}} dv \\ &= \frac{e^{-rT}}{2} - \frac{1}{\pi}\int_0^{\infty} \frac{\mathrm{Im}\left[\psi^{\chi}\left(-i\boldsymbol{v}, \boldsymbol{X}, 0, T\right) e^{i\ln(DK)v}\right]}{\boldsymbol{v}} dv \end{aligned} \tag{4}$$

where $F(0, T, \boldsymbol{X})$ is the price of a forward contract for settlement at time T, derived in Appendix A; $\psi^{\chi}\left(u, \boldsymbol{X}, 0, T\right)$ is the transform function, which is also derived in Appendix A; $i = \sqrt{-1}$, and Im[.] is the imaginary part of a complex number. Note that the intuition behind the functions $G_{1',-1'}(\ln(-DK); \boldsymbol{X}, T, \chi)$ and $G_{0',-1'}(\ln(-DK); \boldsymbol{X}, T, \chi)$ is exactly the same as in the BSM model for the $P_0N(d_1)$ and $N(d_2)$ terms. Thus $G_{1',-1'}(\ln(-DK); \boldsymbol{X}, T, \chi)$ is the expected value of the discounted de-seasonalised spot price, $\exp(X+Y)$, at maturity T, in case it is above the discounted de-seasonalised strike price DK, in the risk-neutral world. Similarly, $G_{0',-1'}(\ln(-DK); \boldsymbol{X}, T, \chi)$ is the risk-neutral probability that the option will be ITM at maturity.

The numerical integration of equations (3) and (4) is carried out using the Adaptive Simpson Quadrature. The main advantage of this procedure is that it is very accurate and fast, as it divides the area of interest in the integration into smaller areas (or intervals), and uses more points in the areas where they are needed and less in the areas that are not needed, since the number of intervals needed does not depend on the behaviour of the integrated function everywhere, but on the points were the function behaves worst; see as well Glasserman, (2004).

---

there is deterministic seasonality the moneyness of the option is directly affected not only by the strike price but also from seasonality.

3 Option Pricing and Moments of the Spike Model

In this section we discuss the impact of the model's parameters on the implied volatility smile generated from the BSM model. For that we will first consider the impact of the model's parameters on the moments of the risk-neutral distribution, i.e. variance, skewness and kurtosis, and then consider the impact of those moments on the implied volatility smile. Any jump-diffusion model will generate a skewed risk-neutral distribution with excess kurtosis. The theoretical variance of daily returns is derived using the characteristic function of the de-seasonalised spot process based on the spike model of equation (1) (as in Das, 2001; see as well Appendix B), and is as follows:

$$Variance = \sigma_X^2 \frac{\left(1-e^{-2k_1\Delta t}\right)}{2k_1} + l\left(\mu_J^2 + \sigma_J^2\right)\frac{\left(1-e^{-2k_2\Delta t}\right)}{2k_2} \qquad (5)$$

The first part of the variance is generated by the normal diffusive variable *X*, and the second from the spike variable *Y*; we call the latter part the *jumpiness*, and it is this part that has the most significant impact on the smile. We can see that the diffusive standard deviation, $\sigma_X\sqrt{\frac{\left(1-e^{-2k_1T}\right)}{2k_1}}$, converges faster to a constant value with k_1 and *T*, rather than increasing continuously with time to maturity as is the case in the BSM formula, $\sigma_X\sqrt{T}$. This implies that, in the absence of jumps, if we calculate the price of a call option using the spike model, and then use the BSM model to find the value of σ such that the BSM option price matches that given by the spike model, we will see that the implied volatility parameter, σ, will be decreasing with time to maturity, as will be shown in later sections. Also as shown in Appendix B, the theoretical skewness and kurtosis of the returns implied from the model are:

$$Skewness = \frac{\frac{l}{3k_2}\left(1-e^{-3k_2\Delta t}\right)\left(\mu_J^3 + 3\mu_J\sigma_J^2\right)}{Variance^{3/2}} \qquad (6)$$

$$Kurtosis = \frac{\frac{l}{4k_2}\left(1-e^{-4k_2\Delta t}\right)\left(\mu_J^4 + 3\sigma_J^4 + 6\sigma_J^2\mu_J^2\right)}{Variance^2} + 3 \qquad (7)$$

where *Variance* is given in equation (5). We can see now that skewness and kurtosis depend exclusively on the parameters of the spike variable. Consider for instance the equation for

skewness, equation (6); since the mean of the jump size, μ_J, is the only parameter that can take negative values, the sign of skewness of the distribution is determined solely by that parameter. This can be explained by the fact that positive (negative) jumps will result in higher (lower) prices which will shift the probability mass to the right (left) and thus induce positive (negative) skewness. Similarly, as the spike-speed of mean-reversion, k_2, increases, the value of skewness and kurtosis decrease. In other words when jumps die-out very fast, i.e. when spikes do not last for long and the market reverts to normal market conditions relatively quickly, the impact of jumps on the skewness and kurtosis is reduced and, *ceteris paribus*, the value of those moments gets closer to 0 and 3, respectively. Furthermore, jump size volatility, σ_J, and frequency, l, also play an important role in determining the size of the skewness and kurtosis of the distribution.

It is then interesting to examine how a change in these moments will affect theoretically the shape of the implied volatility curves. We start by considering the impact of an increase in the variance, while the mean returns remain the same. As a result, the probability mass is shifted from returns close to the centre of the distribution to returns further in the tails; in other words, the distribution curve becomes wider. In terms of options pricing this implies that for all options along the strike price axis the probability of positive payoff increases, which leads to an upward shift of the overall level of the smile curve.

Turning next to the skewness, this determines the relation between the prices of OTM puts and OTM calls. Assuming that the mean and the variance of the spot returns under the risk neutral measure remain constant, consider a decrease in skewness from normality; the probability mass is then shifted from very high to very low prices. The prices of OTM calls, which pay off for high spot prices, thus decrease, and the prices of OTM puts, which have a payoff for low spot prices, increase since there is greater area under the curve at those points. For negative skewness we therefore expect the implied volatility (IV) of OTM puts to be larger than the IV of OTM calls, since the probability of the underlying price reaching low prices is higher than that implied by the BSM model. Consequently, we expect to see a downward sloping smile as shown by Branger (2004) [4].

[4] Note that the term 'downward sloping smile' does not imply a monotonicity of the implied volatility function in a rigorous mathematical sense but rather a general decrease in the shape of IV as we move from ITM to OTM calls.

Finally, kurtosis depends on the fourth moment and measures the fatness of the tails of the distribution. If kurtosis increases, there is more probability mass in the tails of the distribution so very low and very high spot prices both have a higher probability of occurring when compared to the normal distribution. In terms of option pricing, kurtosis is the main driver of the curvature of the smile. Assuming that all other moments remain constant, increasing the kurtosis directly implies higher probability of extreme prices and thus higher prices for OTM puts and OTM calls. In order to hedge against these extreme events, one can form a static portfolio of long positions comprising a continuum of calls with strike prices from zero to infinity, as shown by Carr and Madan (2001).

4 Numerical examination of model Implied Volatilities

Having derived the theoretical equations for the moments of the risk-neutral distribution, the next step is to analyse the spike model's implied volatilities based on the BSM model, which is the anticipated price volatility such that the BSM option price matches the option price given by the spike model of equation (2). More specifically, under the log-normality condition, an option price is a value function of the current spot price *P*, strike *K*, the current time *t* in which the option is evaluated, exercise time *T*, interest rate *r*, and finally, the volatility parameter σ.

$$V_{Option}^{BS} = f_{BS}\left(P, K, t, T, r, \sigma\right)$$

The parameter σ reflects the model's consensus on the anticipated random behaviour of prices on the interval *[t, T]*, i.e. from the current date *t* to the option's maturity date *T*. Now for any given option price from say, the spike model V_{option}^{spike} , the corresponding implied volatility $\sigma^{implied}$ is defined as the value parameter σ, such that:

$$V_{option}^{spike} = f_{BS}\left(P, K, t, T, r, \sigma^{implied}\right) \qquad (8)$$

Applying standard techniques, such as Newton's method, to solve equation (8) we can then obtain the model implied volatility. Our analysis is based on model implied volatilities from the BSM model as this is the benchmark for option pricing and market participants use it back out implied volatilities based on market quotes for option prices. The inconsistency of the BS

model lies on the assumption that the volatility is constant across strike prices and time to maturity and we thus believe that the suggested spike model will be able to capture the volatility smile evidenced in the market.

The use of model implied volatilities is justified by the fact that the exchange-traded options market in Nordpool is illiquid; the majority of option contracts are traded in the over-the-counter market, directly between the counterparties, and for those trades there are no publicly reported prices. Therefore, it is not possible to test, in a reliable way, whether option prices generated from the spike model match the prices of options traded in the market. Such a test requires a continuum of option prices across a range of dates, maturities and strike prices; in addition, in order to ensure that the results are not biased, these options must be liquid and represent traded contracts in the market. Consequently, we focus our analysis on the model implied volatilities relative to the BSM model as this provides the most reliable test for the validity of the spike option pricing model. This analysis will help us identify the major drivers of the volatility smile and also provide valuable insight into the shape of volatilities generated by the spike models and whether the volatilities capture the stylized facts that we anticipate in the market.

Table 1: Parameter values used in the spike model of equation (1)

Model Parameters	Parameters values
$\tilde{\varepsilon}=\left(\varepsilon-\frac{\lambda_X}{k_1}\right)$	5.137
σ_X	0.5
k_1	3
Y_0	0
l	5.5
μ_J	0.1
σ_J	0.283
k_2	290
r	5%

Note: The table shows the parameters of the spike model in equation (1) used for the estimation of European option prices in the base case scenario. See equation (1) for the definition of the variables

In order to calculate the implied volatilities, the spike model is calibrated to Nordpool system prices for the period March 1, 1997 to February 29, 2004 and the estimation results are presented in Table 1 (see Nomikos and Soldatos, 2008 for more details on the estimation process). In the base case, we consider a diffusive volatility of 50% as experimentation with different values showed that this value of volatility creates a more pronounced smile for short-term options - with maturities of less than two months which are examined here. This also helps us identify visually the major contribution of each parameter and generates clearer results for interpretation and discussion.

Since the emphasis of our analysis is on the shape of implied volatilities, we assume that there is no deterministic seasonality, i.e. we assume that $f(t) = 0$. This is because deterministic seasonality affects directly the moneyness of the option, while the shape of the implied volatilities primarily depends on the parameters of the underlying stochastic processes, such as the jump parameters l, μ_J and σ_J and the diffusive volatility σ_X . Therefore, in the following section we analyse the impact that each factor has on the implied volatilities by considering each factor separately, with the following order: First, we examine the effect of mean reversion on implied volatilities. Then, we look at the impact of time to maturity and changes in the mean jump size, μ_J, on the volatility skew. Following that, we explore the comparative impact of the jump intensity, l, against the jump volatility, σ_J, and explore which parameter affects more the curvature of the volatility smile.

Volatility Skew in Mean Reversion

We examine first how the implied volatilities of a pure mean-reverting model look like when the diffusive volatility, σ_X , is 100%, all jump parameters are set to zero and the remaining parameters are as in Table 1. In this analysis we consider short term-to-maturity European options (15 days), and three different equilibrium levels of X; The first case, which we call base case, is when the risk neutral equilibrium level is equal to the current spot price i.e. $\exp\left(\tilde{\varepsilon}\right) = P$; in the second case the equilibrium level is below the current spot price (low case), and finally in the third case the equilibrium level is above the spot price (high case).

These cases reflect different conditions in power markets and, in practice, whether power prices reflect the base, high or low cases considered here depends on a number of factors. In

Nordpool for instance, power prices are usually higher than the long-run yearly average in winter, reflecting the increase in residential demand mainly for heating and lighting purposes, and then drop in the summer as the weather is milder and the days are longer (Lucia and Schwartz, 2002). Another important factor is the generating mix in each power market. In Nordpool about 50% of the electricity is produced using hydro-generators which results in lower power prices. On the other hand, during periods of lower water levels in the reservoirs suppliers have to switch to more expensive fossil-fuel generators with higher marginal cost of production which results in higher system prices. Nomikos and Soldatos (2008) for instance, find that power prices are almost 100 NOK/MWh higher when water reservoir levels are low. Finally, Elliot et al. (2002) also link the level of power prices with the number of generators that are on-line at any given point in time; in the Alberta power pool for instance, they find that when fewer generators are running the price is higher than normal by as much as 70%, while when all the generators are running the price is below the normal price.

Figure 1: Implied volatility of European Call Options across different equilibrium levels
The figure shows the implied volatilities for European Call Options across varying levels of moneyness. We consider three different equilibrium levels corresponding to cases when the risk neutral equilibrium level is equal to the current spot price, $\exp\left(\tilde{\varepsilon}\right) = P$, (Base case), when it is below the current spot price (Low case) and when it is above the current spot price (High case).

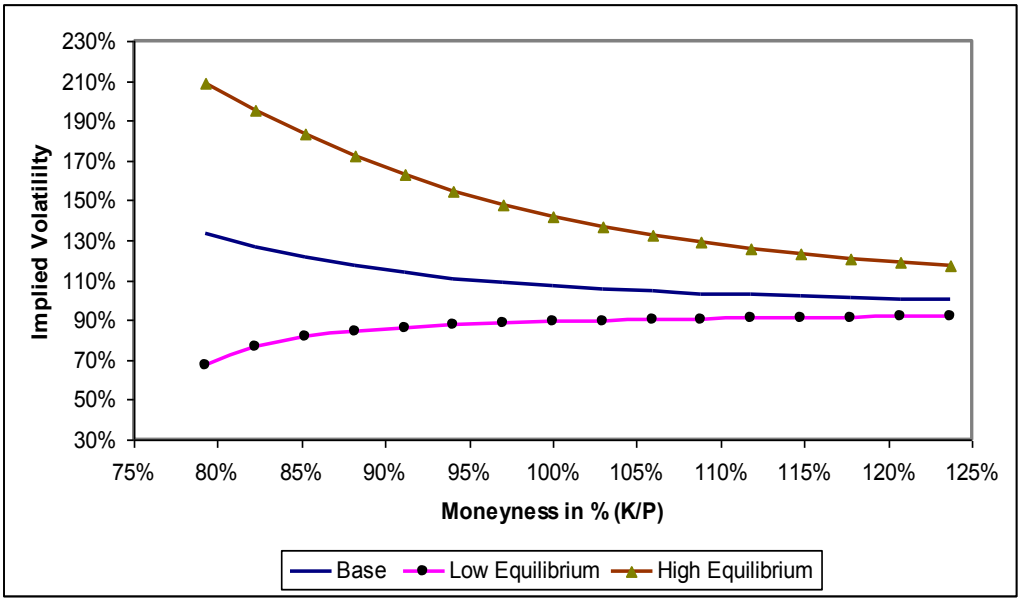

Figure 1 and Figure 2 present the implied volatilities for call and put options, respectively, where moneyness is defined as the ratio K/P. Thus, looking at both figures from left to right,

we are moving from ITM to OTM call options and from OTM to ITM put options. Starting with the call options, we can note that the model displays some degree of skewness reflecting the fact that, due to mean reversion, prices do not fluctuate freely but are pulled back toward their mean. In the base and high cases, where the risk-neutral mean is equal and above the current spot price respectively, mean reversion is good for ITM call options since it pulls prices above the strike price and thus increases the likelihood that the options will end ITM; same is also true for the OTM options, however, since these options have lower probability of ending ITM, the impact of mean reversion is less beneficial compared to ITM options. Overall, this results in the skew evidenced in Figure 1. Turning next to the case where the equilibrium level is below the current spot price (i.e. the low case), we can see that volatility increases as strike price increases. This suggests that prices are now pulled toward lower levels due to mean reversion, and thus ITM calls are cheaper compared to calls calculated using the BSM model. OTM options on the other hand, are less affected by this since they have already a low probability of ending ITM, as the previous results showed. A similar pattern is observed in the case of put options, which are shown in Figure 2, where the implied model volatilities display exactly the opposite pattern from that of call options [5].

[5] The general relationship between the shape of model implied volatilities for call and put options is similar to the one presented in Figure 1 and Figure 2 . In other words positive skewness will decrease IV for OTM Calls and increase IV for OTM Puts. Therefore, in the ensuing analysis we will present only the results for call options. Results for put options are available from the authors.

Figure 2: Implied volatility of European Put Options across different equilibrium levels

The figure shows the implied volatilities for European Put Options across varying levels of moneyness. We consider three different equilibrium levels corresponding to cases when the risk neutral equilibrium level is equal to the current spot price, $\exp\left(\tilde{\varepsilon}\right) = P$, (Base case), when it is below the current spot price (Low case) and when it is above the current spot price (High case).

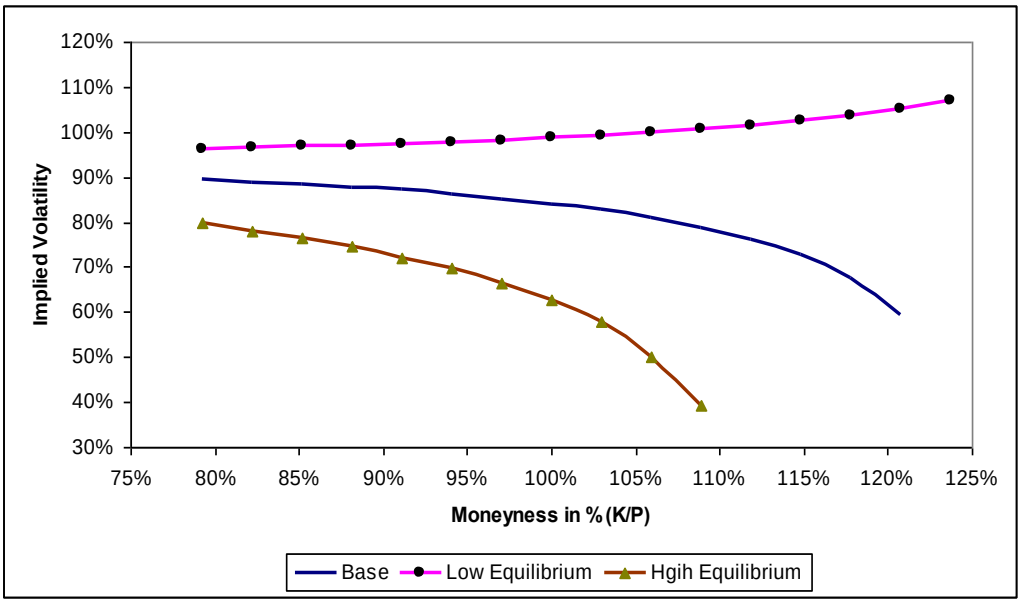

Volatility Smile, Time to Maturity and Mean Reversion

Figure 3 compares the impact of changes in time to maturity on the implied volatilities of the spike model. First thing to note is that as time to maturity increases, implied volatilities decrease which is consistent with the Samuelson Hypothesis and depends on the speed of mean reversion, k_1. This occurs because the BSM model implies that the variance of the spot prices should increase with time to maturity, whereas the variance equation in (5) implies that the variability of the spot prices decreases with time to maturity and eventually converges to a constant value. This also implies that, given that the speed of mean reversion in the spikes is much higher than that in the normal factor X, the contribution to the volatility coming from the spikes is significantly lower than that of the normal process, the longer the maturity of the option. For instance, for short dated options (i.e. 15-days to maturity) the impact of jumps is more pronounced compared to longer-dated ones.

Figure 3: Implied volatility skew of the spike model for 15-day, one and two-month European Call Options.

The figure shows the implied volatilities for European Call Options based on the Spike model using the base case parameters across different strike prices (Moneyness) and maturities (15-days, one- and two-months).

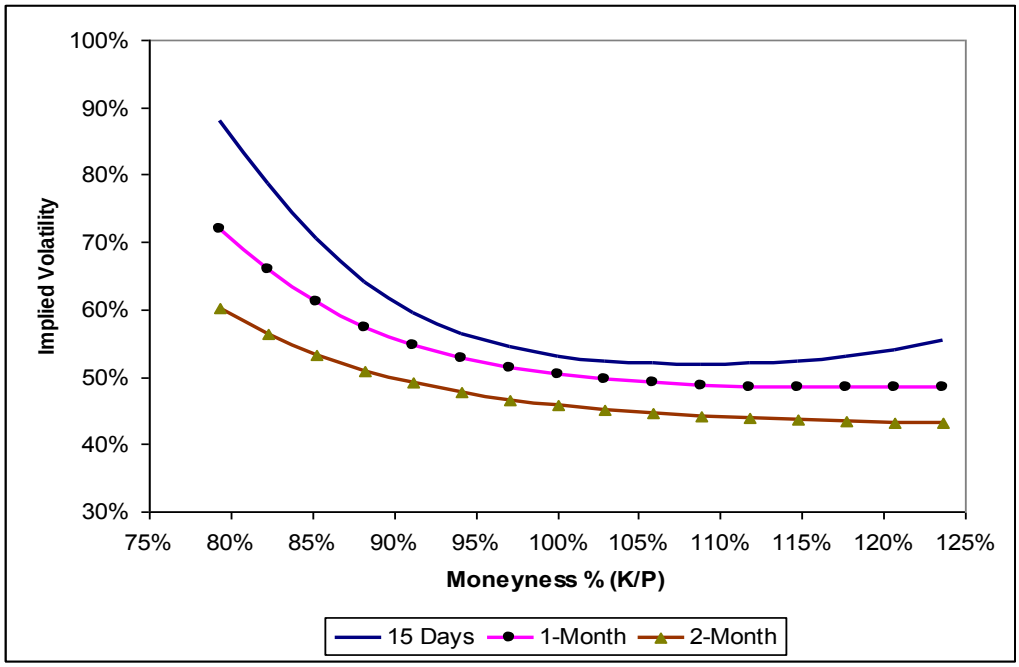

Focusing now on the skewness and kurtosis, it is evident from Figure 3 that there is a pronounced smile for short-term options which then seems to flatten-out, particularly for OTM options, as time to maturity increases [6]. This pattern is consistent with a jump diffusion model and can also be explained by looking at the skewness and kurtosis of the risk neutral distribution in equations (6) and (7). Both moments decrease with time to maturity and speed of mean reversion, and ultimately go to zero (3 for kurtosis) for long enough expiration dates. It seems therefore that the jump diffusion model proposed here produces a pronounced smile for short-term options, and this smile gradually flattens-out out as time-to-maturity increases. This seems to be generally the case with jump diffusion models and, as shown by Rebonato (2004), in order to still have a pronounced smile for long-dated options, it is more appropriate to use a stochastic volatility model as in Heston (1993).

Another important factor affecting the volatility skew is the speed of mean reversion of the diffusive risk, which varies from market to market depending on a number of factors including the power-generation mix of each market. For instance, Escribano et al (2002) show

[6] See Branger (2004) for evidence on how the smile flattens for long maturity options, when using Merton's (1976) model.

that the degree of mean reversion in hydro-markets is lower than that evidenced in fossil-fuel based power markets, since hydro reservoirs play the role of indirect storage of electricity; as a result, there is some inter-temporal substitution for generating electricity which can dampen short-term variations in power prices, thus lowering the coefficient of mean reversion. In markets with no inter-temporal substitution, on the other hand, we should observe a higher degree of diffusive mean-reversion since generators cannot use inventories to smooth-out shocks, and the degree of mean reversion in electricity prices is mainly driven by the mean reversion in demand or in temperature. Along the same lines, Elliot et al. (2002) also show that there is a link between the number of generators and the degree of mean reversion; when fewer generators are running, and thus when prices are higher, the degree of mean reversion is higher, compared to when all the generators are running and thus there is spare capacity in the market.

As the speed of mean reversion of the diffusive risk, k_1, increases, we expect a similar pattern to that observed in Figure 3. In particular, the higher the value of k_1, the faster the volatility will converge to a constant value and thus the lower the implied volatility. Similarly, we expect a more pronounced smile the slower the speed of mean reversion (i.e. for lower values of k_1) and the smile will gradually flatten-out as the speed of mean reversion increases. Therefore, an increase in the speed of mean reversion will have a similar impact on implied volatilities as that of increasing the time-to-maturity of the option and vice-versa.

Volatility smile and mean Jump Size

Spikes are a prominent feature of power prices and are one of the most important factors affecting the volatility skew. The sign and size of expected jumps in power markets depend on a number of factors. For instance, Nomikos and Soldatos (2008) find very strong evidence of seasonality in the spikes in the Nordpool market. Upward spikes occur mainly during winter and are larger on average, since in winter the market operates at the steep part of the supply stack which, combined with any outage or transmission failure, may cause extreme price movements. Negative spikes, on the other hand, occur mainly during the spring and summer periods and non-working days and also appear to be smaller, in absolute terms. The size of spikes also depends on the power generation-mix in the market. For instance, in markets where electricity is generated by fossil fuel technology, prices are more volatile and spikes are more frequent and larger compared to markets where hydroelectricity is used (Escribano et al., 2002)

Figure 4: Implied volatility skew for 15-Day Call Options with respect to the sign of mean jump size μ_J

The figure shows the implied volatilities for European Call Options with 15-days to maturity based on the spike model across different strike prices (Moneyness), using positive and negative mean jump sizes, μ_J, and the remaining parameters being the same as in the base case, in Table 1.

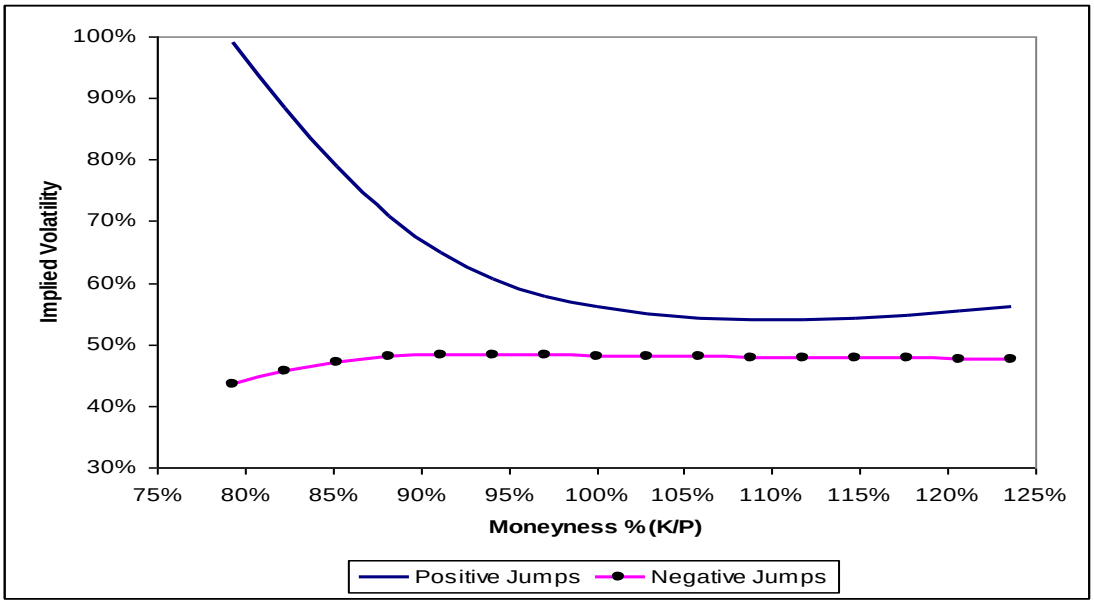

As shown in equation (6), the sign of skewness depends on the sign of the expected jumps $E\left[Jdq(l)\right]$ in log-returns, a fact that is depicted in Figure 4. If μ_J is negative, the volatility smile seems to be upward slopping when moving from ITM to ATM call options and then becomes relatively flat, reflecting the fact that in this case there is a higher probability, than that implied from a normal distribution, for prices to reach very low levels. Similarly, when jumps are positive, the volatility smile is downward sloping as we move from ITM to ATM call options. It is worth noting that the pattern evidenced here is the opposite of what would have been expected using an ordinary jump diffusion model - e.g. without mean reversion in the jumps, such as Merton's (1976) - where a positive jump would result in OTM call options to have higher implied volatilities than ATM and ITM options. However, this is not generally the case when mean reversion is incorporated in the model. Mean reversion pulls prices back to their equilibrium level which, in the base case considered here, is equal to the spot rate and thus, higher than the exercise price of ITM call options and lower than the exercise price of OTM call options. This reduces the probability of OTM calls ending up ITM and, at the same time, ITM call options have a higher probability of ending more ITM compared to an ordinary jump-diffusion model. Therefore, in the presence of positive jumps we expect to see implied

volatilities which decrease in an exponential fashion with strike prices, thus producing the negative skew shown in the graph. In the case of negative jumps, the probability mass is shifted to lower spot prices compared to the earlier case, which reduces the probability of call options to end ITM and results in lower implied volatilities. OTM options, on the other hand, are less affected by this since, due to mean reversion in prices, the probability of profitable exercise is already low.

Volatility smile curvature; Jump intensity versus Jump size volatility

Finally, we analyse the impact of jumpiness, which is the contribution of the jump component in the total variance as shown in equation (5). A jump diffusion model can be interpreted as a mixture of a pure jump process, as in the spike variable Y, and a diffusive process such as a GBM or a mean reversion. The issue is then to examine the impact of jumpiness on the smile and whether this is affected differently by changing each of the constituent components of jumpiness, namely σ_J and l. The two extreme cases are when the jumpiness is zero and the implied volatilities for OTM options become flat, and when the jumpiness is one in which case the smile has the maximum curvature.

Figure 5: Implied Volatility Skew for 15-Day European Call Options for different levels of jumpiness due to changes in Jump size volatility σ_J

The figure shows the implied volatilities for European Call Options with 15-days to maturity for the Spike model across different levels of moneyness, by changing the contribution of jumpiness to the total variance with respect to σ_J and all other parameters remaining the same as in the base case, in Table 1.

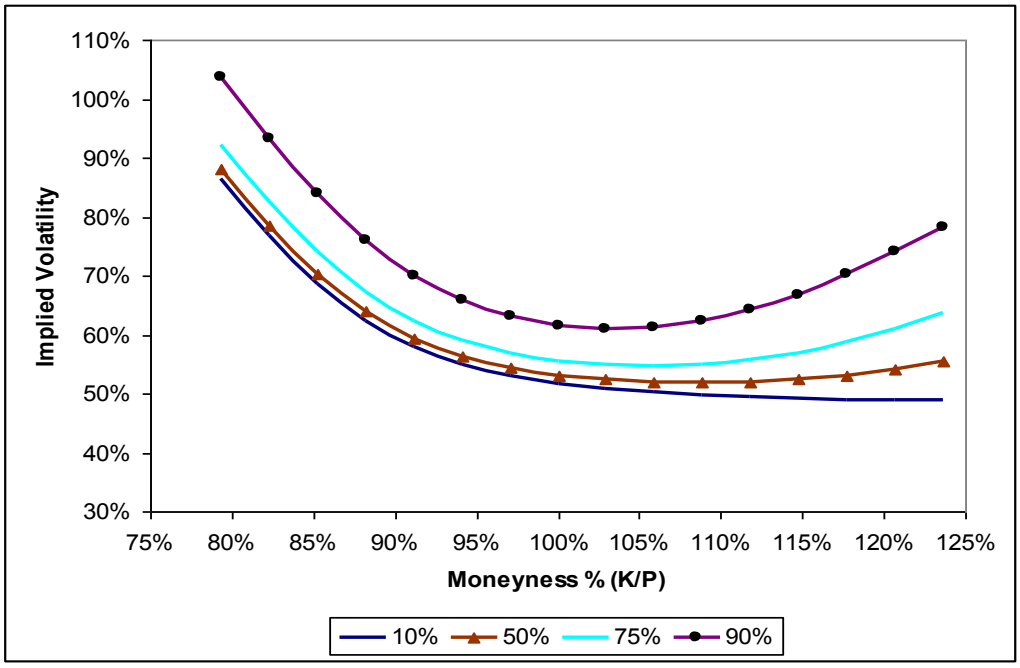

Figure 5 displays the implied model volatilities for different levels of jumpiness, expressed as the percentage of the total volatility given in equation (5), by changing the jump size volatility, σ_J, for options that are 15-days to maturity. For instance, a 90% jumpiness level means that jumpiness accounts for 90% of the total variance in equation (5) and this is achieved by changing the jump volatility, σ_J, whilst keeping the jump intensity, *l*, the same as in the base case. We can see that that the smile becomes more pronounced as jumpiness increases and the implied volatilities of course are higher, since the overall volatility increases.

Figure 6: Implied Volatility Skew for 15-Day European Call Options for different levels of jumpiness due to changes in Jump intensity *l*

The figure shows the implied volatilities for European Call Options with 15-days maturity for the Spike model across different levels of moneyness, by changing the contribution of jumpiness to the total variance with respect to *l* and all other parameters remaining the same as in the base case, in Table 1.

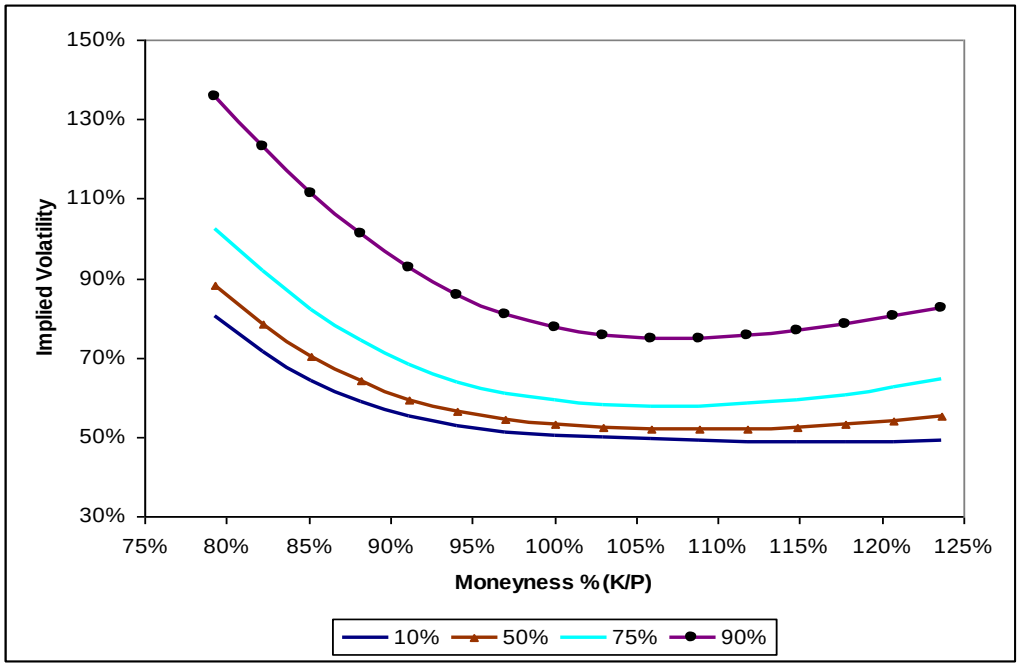

Similar conclusions emerge when we examine Figure 6 which presents the implied volatilities for different levels of jumpiness, when increasing the jump intensity, *l*. Comparing the same levels of jumpiness, between Figure 5 and Figure 6, we note that when the increase in the contribution of jumpiness is due to an increase in jump-size volatility, the smile appears to be more pronounced than when it is due to an increase in jump-intensity. This is also evident in Table 2, where we report the percentage change in the parameters required in order to achieve a given level of jumpiness. We see that as the total contribution of the jumpiness increases,

the required percentage increase in intensity from the base case becomes very large; e.g. l needs to increase by 800% from the base case in order to achieve 90% jumpiness, whereas the comparative increase for jump size volatility is 216%. It seems therefore that jump size volatility plays a more important role in affecting the jumpiness and thus the kurtosis of implied volatilities.

Table 2: Required percentage change in σ_J or l in order to achieve a given level of jumpiness

This table shows the required percentage change in jump size volatility, $\boldsymbol{\sigma_J}$, or jump intensity, $\boldsymbol{l}$, compared to the base case (50% jumpiness), in order to reach a given level of jumpiness.

Jumpiness	***10%***	***25%***	***50%***	***75%***	***90%***
$\boldsymbol{\sigma_J}$	-99.59%	-50.00%	0%	80.28%	216%
$\boldsymbol{l}$	-88.89%	-66.67%	0%	200%	800%

Another method for assessing whether it is the jump size volatility or intensity that contributes more to the smile curvature, is to employ the following three scenarios; one is the base case, using the same parameters as in Table 1, where jumpiness in equation (5) accounts for 50% of the total variance; in the second case, jump intensity is doubled in size and thus jump size volatility is lowered in order to keep the jumpiness at 50%, and in the third case, jump size volatility is doubled and jump intensity is lowered thus keeping again the jumpiness at 50%. The results are presented in Figure 7.

We can see that when jump intensity, l, doubles, the overall level of implied volatilities increases and there is still a pronounced smile, but the slope of the volatility curve (mainly for OTM call options) is lower (i.e. flatter) compared to when doubling σ_J. This is also consistent with the analysis presented in Figure 5 and Figure 6, which indicates that the smile is more pronounced when changes in jumpiness are due to changes in jump-size volatility. Thus, by keeping the spot returns' volatility constant, if the jump volatility is reduced and this is offset by an increase in jump intensity, then the excess kurtosis of the distribution is reduced, making the smile flatter. On the other hand, if an increase in jump size volatility goes together with a decrease in jump arrivals, the smile becomes more pronounced due to an increase in the kurtosis. In all cases ITM volatilities are higher again due to mean reversion.

Of course we would also expect similar results for put options; in this case, the shape of the volatility smile is exactly the opposite from that of call, but the intuition remains the same.

Figure 7: Implied volatility Skew for 15-Day European Call Options with respect to Jump Intensity *l* and Jump Volatility σ_J

The figure shows the implied volatilities generated from the spike model, when increasing by 100% either the jump size volatility or the jump intensity, but always keeping the overall level of jumpiness at 50%.

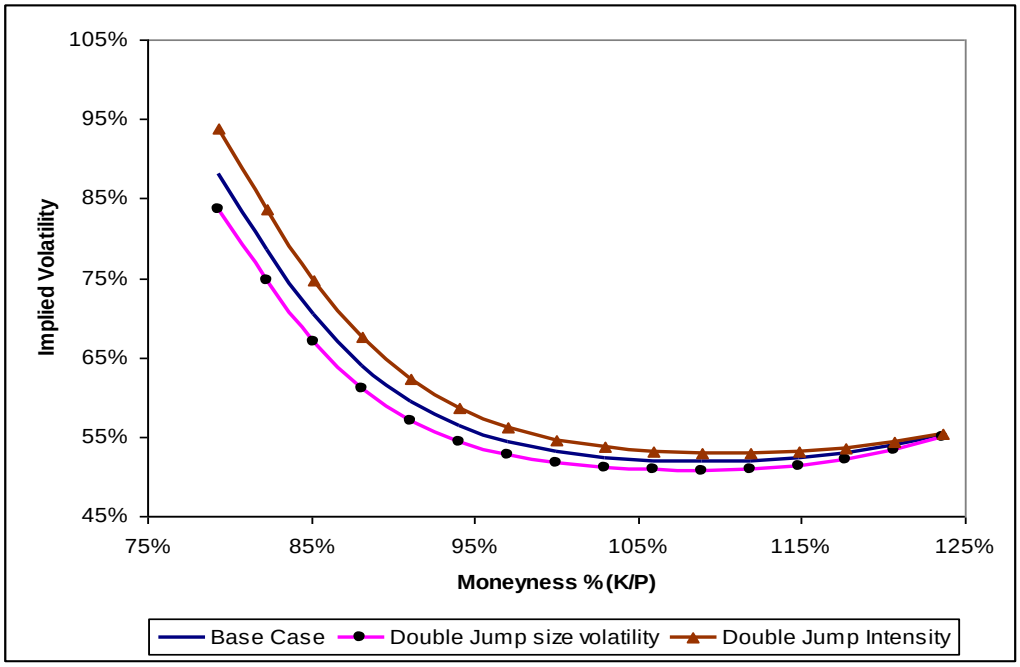

5 Conclusions

In this paper we derived semi closed-form solutions for European options using a spike model. The model is flexible in its formulation and captures the stylized features of power prices. The main feature of the model is that it incorporates two different speeds of mean reversion: one for the diffusive part of the model and another one for the spikes, with the latter being much higher than the former in order to capture the fast decay of jumps in the market and the fact that spikes affect spot prices and do not spill-over to the forward market. We derive semi-closed form solutions using the transform analysis by Duffie et al (2001) and provide an intuitive explanation on each of the terms of the pricing equation. To provide further insight on the option pricing model, we calibrate the model in the Nordpool market and then calculate option prices which are used as inputs in the Black-Scholes-Merton model in order to extract implied volatilities. We find that the presence of jumps generates prominent volatility skews which depend on the sign of the mean jump size. We also show

that mean reversion reduces the volatility smile as time to maturity increases; interestingly, we find that even in the absence of jumps, mean reversion induces volatility skews particularly for ITM options. Finally, jump size volatility and jump intensity mainly affect the kurtosis and thus the curvature of the smile with the former having a more important role.

There are several implications based on these results. First, in a mean-reverting market, a participant using a GBM model will get misleading results; for instance, if the spot price is above the equilibrium price, a mean reverting model will price an ATM call closer to an OTM taking into account the fact that the price will have the tendency to revert to its equilibrium price, thus reducing the probability of ending ITM. On the other hand, the presence of jumps increases the probability of OTM options ending ITM, thus making exercise more likely; for instance, positive jumps will increase the values of OTM calls and negative jumps will increase the values of OTM puts. However, the overall impact of jumps on option prices will also depend on the spike-speed of mean reversion as well as the time-to-maturity of the option since the impact of jumps is higher for short-term options. Overall, an increase in the intensity and volatility of jumps will increase the price of OTM calls and puts, when compared to the Black-Scholes-Merton model.

6 REFERENCES

Bessembinder, H. and Lemmon, M.L., (2002), "Equilibrium Pricing and Optimal Hedging in Electricity Forward Markets", *Journal of Finance* 57, 1347-82.

Black, F. (1976). The Pricing of Commodity Contracts. *Journal of Financial Economics*, vol (3), 167-169

Black, F. and Scholes, M. (1973), "The Pricing of Options and Corporate Liabilities*"*, *Journal of Political Economy*, 673-54.

Branger, N., (2004), "An Option Pricing Anatomy", Working Paper

Carr, P., and Madan, D., (2001), "Optimal Positioning in Derivatives Pricing", *Quantitative Finance*, 1, 19-37

Cerny, A., (2009), "*Mathematical Techniques in Finance*", Princeton University Press, Oxford, UK

Chacko, G. and Das, S., (2002), "Pricing Interest Rate Derivatives: A General Approach", *Review of Financial Studies*, 15(1), 195-241.

Clewlow, L., and Strickland, C., (2000), "*Energy derivatives: Pricing and Risk Management"*, Lacima Publications.

Dai, Q. and Singleton, K.J. (2000), "Specification analysis of affine term structure models" *Journal of Finance,* Vol. 55, N° 5, 1943-1978.

Das, S.D., (2001),"The Surprise Element: Jumps in Interest Rates", *Journal of Econometrics,* 106, 27-65.

Duffie, D., Pan, J. and Singleton, K. (2000) "Transform analysis and asset pricing for affine jump-diffusions", *Econometrica,* vol. 68(6), 1343-1376.

Elliott, R.J., Sick, G. and Stein, M (2002), "Price Interactions of Baseload Supply Changes and Electricity Demand Shocks", in *Real Options and Energy Management,* Ed. Ronn, E., Risk Books, London, 371-391.

Escribano, A., Peña, Juan. I. and Villaplana, P., (2002). "Modelling Electricity Prices: International Evidence," Economics Working Papers, we022708, Universidad Carlos III, Departamento de Economía.

Ethier, S., and Kurtz, T., 1986, "*Markov Processes, Characterization and Convergence"*, New York: John Willey & Sons

Geman, H. and Roncoroni, A., 2006, "Understanding the Fine Structure of Electricity Prices", *Journal of Business,* Vol. 79, No. 3.

Geman, H., 2005, "*Commodities and commodity derivatives: Modelling and Pricing for Agriculturals, Metal and Energy*" (Wiley Finance).

Glasserman, P., (2004), "*Monte Carlo Methods in Financial Engineering*", Stochastic Modelling and Applied Probability, Springer Finance.

Heston, S. (1993). "A Closed-Form Solution of Options with Stochastic Volatility with Applications to Bond and Currency Options", *Review of Financial Studies,* 6, 327-343.

Huisman, R., (2009), "*An Introduction to Models for the Energy Markets*", Risk Publications, London, UK.

Longstaff, F., and Wang, A., (2002), "Electricity Forward Prices: a high-frequency empirical analysis", Working Paper, UCLA

Lucia, J. and E. Schwartz, (2002), "Electricity prices and power derivatives. Evidence from Nordic Power Exchange", *Review of Derivatives Research,* vol. 5 (1), 5-50.

Merton R, (1973), "Theory of Rational Option Pricing," *Bell Journal of Economics and Management Science* 4:1, 141 – 183.

Merton R, (1976), "Option pricing when underlying stock returns are discontinuous," *Journal of Financial Economics* 3, 125-144.

Nomikos N, and Soldatos, O. (2008), "Using Affine Jump Diffusion Models for Modelling and Pricing Electricity Derivatives", *Applied Mathematical Finance,* 15(1), p.41-71

Rebonato, R., (2004), "*Volatility and Correlation: the Perfect Hedger and the Fox*", Wiley, NY.

Samuleson, P. (1965) “Proof that properly anticipated prices fluctuate randomly”, *Industrial Management Review*, 6, 13 - 31.

Schwartz, E. and Smith, J.E., (2000), “Short-term variations and long-term dynamics in commodity prices”, *Management Science*, 46 (7), 893-911.

Vasicek, O., 1977, “An Equilibrium Characterization of the term structure”, *Journal of Finance* 5, 177-188.

Villaplana, P., (2003), “Pricing Power Derivatives: A Two Factor Jump-Diffusion approach, Working Paper, Universitat Pompeu Fabra.

Weron, R., (2008), “Market price of risk implied by Asian-style electricity options and futures”, *Energy Economics*, Vol 30, 3, May, 1098 - 1115.

7 Appendix A: Introduction and Application of the Transform Function for the Forward Prices in the Factor Model

A very useful assumption in the finance literature is that the state vector *X* follows an affine jump-diffusion process (AJD). An AJD is a jump-diffusion process for which the drift vector, the "instantaneous" covariance matrix, and jump intensities all have an affine (i.e. linear) dependence on the state vector. The affine jump-diffusion processes have been synthesized and extended by Duffie et al. (2000) (henceforth DPS); see also Chacko and Das (2002) and Dai and Singleton (2000). Affine diffusions (AD) and affine jump-diffusions (AJD) processes are quite useful in modelling underlying state variable due to their flexibility and tractability. DPS, for instance, have shown the close connection between the structure of affine models and Fourier transforms, and demonstrate how from this transform one can obtain derivative prices. The jump diffusion model presented in the main body of the paper belongs to the class of AJD. Hence, we can use the results provided by DPS in their transform analysis to obtain closed-form solutions implied by the spike model for forward and option prices.

The DPS transform can be described as follows: Fix a probability space $\{\Omega, \mathcal{F}, P\}$ and an information filtration $(\mathcal{F}_t) = \{\mathcal{F}_t : t \geq 0\}$, and suppose that $\boldsymbol{X}_t$ is a Markov process in some state space $D \subset \mathbb{R}^n$, following the stochastic differential equation (SDE):

$$d\boldsymbol{X}_t = \mu(\boldsymbol{X}_t)dt + \sigma(\boldsymbol{X}_t)dW_t + dZ_t \qquad (9)$$

Where W_t is an $(\mathcal{F}_t)$-standard Brownian motion in $\mathbb{R}^n$; $\mu(.): D \to \mathbb{R}^n$, $\sigma(.): D \to \mathbb{R}^{n \times n}$ are respectively the drift and diffusion functions, and Z_t is a pure jump process whose jump sizes have a fixed probability distribution v on $\mathbb{R}^n$ and arrive at frequency $\{l(\boldsymbol{X}_t) : t \geq 0\}$ for some $l: D \to [0, \infty)$. To be precise, suppose that $\boldsymbol{X}_t$ is a Markov process whose transition semi-group

has an infinitesimal generator $\mathcal{D}$ of the Lèvy type, [7] defined at a bounded C^2 function $f: D \to \mathbb{R}$, with bounded first and second derivatives, by

$$\mathcal{D} f(\boldsymbol{x},t) = f_t(\boldsymbol{x},t) + f_{\boldsymbol{x}}(\boldsymbol{x},t)\mu(\boldsymbol{x}) + \frac{1}{2} tr\left[f_{\boldsymbol{xx}}(\boldsymbol{x},t)\sigma(\boldsymbol{x})\sigma(\boldsymbol{x})^T \right] + l(\boldsymbol{x})\int_{\mathbb{R}} \left[f(\boldsymbol{x}+z,t) - f(\boldsymbol{x},t) \right] dv(z) \tag{10}$$

Intuitively, $\mu(\boldsymbol{X}_t)$ and $\sigma(\boldsymbol{X}_t)$ are the drift and diffusion terms of the process when no jump occurs, and the jump term captures the discontinuous change of the path with both random arrival of jumps and random jump sizes. That is, conditional on the path of $\boldsymbol{X}$, the jump times of the jump term are the jumps times of a Poisson process with, possibly, time-varying intensity $\{l(\boldsymbol{X}_s): 0 \le s \le t\}$, and the size of the jump at a jump time m is independent of $\{\boldsymbol{X}_s : 0 \le s \le m\}$ and has the probability distribution v.

In order for the transform function to work, as stated by DPS (2000), the drift, variance-covariance, intensity and discount rate have to be affine functions of the state variables, hence:

$$\begin{aligned}
&\mu(\boldsymbol{x}) = K_0 + K_1 \bullet \boldsymbol{x}, \text{ for } K = (K_0, K_1) \in \mathbb{R}^n \times \mathbb{R}^{n \times n}. \\
&\left(\sigma(\boldsymbol{x})\sigma(\boldsymbol{x})^T\right)_{ij} = \left(H_0\right)_{ij} + \left(H_1\right)_{\mathrm{ij}} \bullet \boldsymbol{x}, \text{ for } H = (H_0, H_1) \in \mathbb{R}^{n \times n} \times \mathbb{R}^{n \times n \times n}. \\
&l(\boldsymbol{x}) = l_0 + l_1 \bullet \boldsymbol{x}, \text{ for } l = (l_0, l_1) \in \mathbb{R} \times \mathbb{R}^n. \\
&R(\boldsymbol{x}) = \rho_0 + \rho_1 \bullet \boldsymbol{x}, \text{ for } \rho = (\rho_0, \rho_1) \in \mathbb{R} \times \mathbb{R}^n.
\end{aligned} \tag{11}$$

Let $\theta(c) = \int_{\mathbb{R}^n} \exp\{c \times z\}\, dv(z)$, be the characteristic function of the jump size distribution. The function $\theta(\bullet)$ determines completely the jump size distribution. Also assuming constant interest rates, $R(\boldsymbol{x}) = \rho_0$, futures prices are equal to forward prices. Let $\chi \equiv (K, H, l, \rho, \theta)$ which captures both the distribution of the vector process $\boldsymbol{X}$ as well as the effects of

[7] The generator $\mathcal{D}$ is defined by the property that $\{ f(\boldsymbol{X}_t, t) - \int_0^t \mathcal{D} f(\boldsymbol{X}_s, s) ds : t \ge 0\}$ is a martingale for any f in its domain (Ethier and Kurtz, 1986).

discounting, and determines a transform ψ^{χ}: $\mathbb{C}^n \times D \times \mathbb{R}_+ \times \mathbb{R}_+ \to \mathbb{C}$ of $\boldsymbol{X}_T$ conditional on $\mathcal{F}_t$, when well defined at $t \le T$, by

$$\psi^{\chi}(u, \boldsymbol{X}_t, t, T) = E^{\chi}\left[\exp\left(-\int_t^T R(\boldsymbol{X}_s)ds\right)e^{u \bullet \boldsymbol{X}_T} \mid \mathcal{F}_t\right] \tag{12}$$

Where E^{χ} denotes the expectation operator under the distribution of $\boldsymbol{X}$ determined by χ. Hence the difference between the conditional characteristic function of $\boldsymbol{X}_T$ and the transform function ψ^{χ} is the discount factor $R(\boldsymbol{X}_T)$. Therefore, under technical regularity conditions DPS (2000) show that

$$\psi^{\chi}(u, \boldsymbol{X}_t, t, T) = e^{\alpha(t)+\beta(t)\bullet x} \tag{13}$$

Where α and β satisfy the following complex-valued Ordinary-Differential-Equations:

$$\begin{aligned}
\dot{\beta}(t) &= \rho_1 - K_1^T\beta(t) - \frac{1}{2}\beta(t)^T H_1\beta(t) - l_1\left(\theta\left(\beta(t)\right)-1\right), \\
\dot{\alpha}(t) &= \rho_0 - K_0^T\beta(t) - \frac{1}{2}\beta(t)^T H_0\beta(t) - l_0\left(\theta\left(\beta(t)\right)-1\right)
\end{aligned} \tag{14}$$

With boundary conditions $\alpha(T)=0$ and $\beta(T)=u$.

Application to the Spike Model

Now for the Spike model of equation (1) with constant jump parameters, the connection between the transform function and its use to find the forward prices is as follows:

$$\begin{aligned}
P_t &= f(t) + \exp\left(X_t + Y_t\right) \\
dX_t &= \left(-\lambda_X + k_1\left(\varepsilon - X_t\right)\right)dt + \sigma_X dW_X^* \\
dY_t &= -k_2 Y_t dt + J(\mu_J, \sigma_J^2)dq(l)
\end{aligned} \tag{15}$$

Therefore,

$$\begin{aligned}
E_t^*\left(P_T - f(T)\right) &= e^{r\tau}E_t^*\left(e^{-r\tau}\exp\left(X_T + Y_T\right)\right) = e^{r\tau}\psi^{\chi}(u, \boldsymbol{X}_t, t, T) \\
&= e^{r\tau}\exp(\alpha(t) + \beta_1(t) \bullet X + \beta_2(t) \bullet Y)
\end{aligned} \tag{16}$$

Where the vectors $u=(1,1)$, and $\boldsymbol{X} = (X_t, Y_t)$ and $\tau=T-t$.

From (16) we use (14) to reach to the Ordinary Differential Equations and solve them:

$$\frac{\partial \beta_i}{\partial t} = k_i \beta_i \text{ and } \beta_i(T) = 1 \Rightarrow \beta_i(t) = e^{-k_i \tau}$$
$$\text{Hence } \beta_1(t) = e^{-k_1 \tau},\ \beta_2(t) = e^{-k_2 \tau} \tag{17}$$

$$\theta(\beta_2(t)) = \exp\left(\mu_J e^{-k_2(T-s)} + \frac{1}{2}\sigma_J^2 e^{-2k_2(T-s)} \right)$$

$$\alpha(t) = \int_t^T r + \left(\lambda_X - k_1 \varepsilon\right) e^{-k_1(T-s)} - \frac{1}{2} e^{-2k_1(T-s)} \sigma_X^2 - l\left(\exp\left(\mu_J e^{-k_2(T-s)} + \frac{1}{2}\sigma_J^2 e^{-2k_2(T-s)} \right) - 1 \right) ds$$

Hence, using equation (16) and the results from equation (17), we have the expected value of the spot under the risk neutral probability measure:

$$E_0^*(P_t) = f(t) + \exp\left(e^{-k_1 t} X_0 + Y_0 e^{-k_2 t} + l \int_0^t \left(\exp\left(\mu_J e^{-k_2 s} + \frac{1}{2}\sigma_J^2 e^{-2k_2 s} \right) - 1 \right) ds + A_t \right)$$
$$A_t = \frac{1}{2}\frac{\sigma_x^2}{2k_1}\left(1 - e^{-2k_1 t}\right) + \left(\varepsilon - \frac{\lambda_x}{k_1} \right)\left(1 - e^{-k_1 t}\right) \tag{18}$$

Using then equation (18) we define the de-seasonalised price of a forward contract for settlement at time *T* as follows:

$$F(0, T, \boldsymbol{X}) = E_0^*(P_T) - f(t) \tag{19}$$

Proof of the formula for the security price $G_{a,b}(y)$

For $0 < \tau < \infty$ and a fixed $y \in \mathbb{R}$,

$$\frac{1}{2\pi}\int_{-\tau}^{\tau} \frac{e^{ivy}\psi^{\chi}\left(a - ivb, \boldsymbol{X}, 0, T\right) - e^{-ivy}\psi^{\chi}\left(a + ivb, \boldsymbol{X}, 0, T\right)}{iv} dv$$
$$= \frac{1}{2\pi}\int_{-\tau}^{\tau}\int_{\mathbb{R}} \frac{e^{-iv(z-y)} - e^{iv(y-z)}}{iv} dG_{a,b}(z; \boldsymbol{X}, T, \chi) dv$$
$$= -\frac{1}{2\pi}\int_{\mathbb{R}}\int_{-\tau}^{\tau} \frac{e^{-iv(z-y)} - e^{iv(y-z)}}{iv} dv dG_{a,b}(z; \boldsymbol{X}, T, \chi)$$

where *Fubini* is applicable because: $\lim_{y\to\infty} G_{a,b}\left(y; \boldsymbol{X}, T, \chi\right) = \psi^{\chi}\left(a, \boldsymbol{X}, 0, T\right) < \infty$ given that χ is well defined at *(α,T)*. Next, we note that for $\tau > 0$,

$$\int_{-\tau}^{\tau} \frac{e^{-iv(z-y)} - e^{iv(y-z)}}{iv} dv = -\frac{\operatorname{sgn}(z-y)}{\pi} \int_{-\tau}^{\tau} \frac{\sin\left(v|z-y|\right)}{v} dv$$

is bounded simultaneously in z and τ, for each fixed y. By the bounded convergence theorem,

$$\begin{aligned}
&\lim_{\tau\to\infty} \frac{1}{2\pi} \int_{-\tau}^{\tau} \frac{e^{ivy}\psi^{\chi}\left(a - ivb, \boldsymbol{X}, 0, T\right) - e^{-ivy}\psi^{\chi}\left(a + ivb, \boldsymbol{X}, 0, T\right)}{iv} dv \\
&= -\int_{\mathbb{R}} \operatorname{sgn}(z-y) dG_{a,b}\left(z; \boldsymbol{X}, T, \chi\right) \\
&= -\psi^{\chi}\left(a, \boldsymbol{X}, 0, T\right) + \left(G_{a,b}\left(y; \boldsymbol{X}, T, \chi\right) + G_{a,b}\left(y-; \boldsymbol{X}, T, \chi\right)\right)
\end{aligned}$$

where $G_{a,b}\left(y-; \boldsymbol{X}, T, \chi\right) = \lim_{z\to y, z\le y} G_{a,b}\left(z; \boldsymbol{X}, T, \chi\right)$. Using the integrability condition $\int_{\mathbb{R}} \left|\psi^{\chi}\left(a + ivb, \boldsymbol{X}, 0, T\right)\right| dv < \infty$, and by the dominated convergence theorem we have

$$G_{a,b}\left(y; \boldsymbol{X}, T, \chi\right) = \frac{\psi^{\chi}\left(a, \boldsymbol{X}, 0, T\right)}{2} + \frac{1}{4\pi} \int_{-\infty}^{\infty} \frac{e^{ivy}\psi^{\chi}\left(a - ivb, \boldsymbol{X}, 0, T\right) - e^{-ivy}\psi^{\chi}\left(a + ivb, \boldsymbol{X}, 0, T\right)}{iv} dv$$

Because $\psi^{\chi}\left(a - ivb, \boldsymbol{X}, 0, T\right)$ is the complex conjugate of $\psi^{\chi}\left(a + ivb, \boldsymbol{X}, 0, T\right)$ we have

$$G_{a,b}\left(y; \boldsymbol{X}, T, \chi\right) = \frac{\psi^{\chi}\left(a, \boldsymbol{X}, 0, T\right)}{2} + \frac{1}{\pi} \int_{0}^{\infty} \frac{e^{-ivy}\psi^{\chi}\left(a + ivb, \boldsymbol{X}, 0, T\right)}{iv} dv$$

8 Appendix B: Closed-form Solutions of the Moments of the Spike Model

As shown by Das (2001), one can obtain closed-form solutions of the moments of any jump distribution by first deriving the characteristic function, $F(\boldsymbol{X}, t, T; s)$, given that the jump intensity or jump distribution does not depend on the state variables. The solution of the characteristic function can be found using the DPS transform as follows:

$$F(\boldsymbol{X},T,t,T=t;s) = exp(is(X+Y))$$

where $\boldsymbol{X}=(X,Y)$. The above equation is also the boundary condition for the characteristic function. The relation between the characteristic function and the transform is given by:

$$\psi^{\chi}(u,\boldsymbol{X}_t,t,T) = e^{-r\tau}F\left(X,Y,T;s\right) \qquad (20)$$

where $u=(is, is)$. Therefore, the solution of the characteristic function takes the form of the transform:

$$F\left(X,Y,t,T;s\right) = \exp(\alpha(t)+\beta_1(t)\bullet X+\beta_2(t)\bullet Y) \qquad (21)$$

with boundary conditions $a(T) = 0$, $\beta_1(T) = \beta_2(T) = is$. Thus, using the results from the transform analysis, and letting $\tau=T-t$:

$$\frac{\partial\beta_i}{\partial t} = k_i\beta_i \text{ and } \beta_i(T) = is \Rightarrow \beta_i(t) = ise^{-k_i\tau}$$

Hence $\beta_1(t) = ise^{-k_1\tau}$, $\beta_2(t) = ise^{-k_2\tau}$

$$a(t) = r\tau + \left(is\right)^2\frac{1}{2}\frac{\sigma_X^2}{2k_1}\left(1-e^{-2k_1\tau}\right) + is\varepsilon(1-e^{-k_1\tau}) + l\int E\left(\exp(isJe^{-k_2\tau})-1\right)d\tau$$

Now in order to find closed-form solutions for the moments, we need to differentiate the characteristic function successively with respect to s and then find the value of the derivative when $s=0$. Thus, if we denote the n^{th} moment by m_n, and the n^{th} derivative of the characteristic function by $F_n = \partial^n F/\partial s^n$, the moments can be derived using

$m_n = 1/i^n \left[F_n \middle| s=0 \right]$. However, since the characteristic function F, depends on α and β, we first have to derive their derivatives with respect to s. The derivatives of β with respect to s are as follows:

$$\frac{d\beta_i}{ds} = ie^{-k_i\tau}, \quad \frac{d^2\beta_i}{ds^2} = \frac{d^3\beta_i}{ds^3} = \frac{d^4\beta_i}{ds^4} = 0 \tag{22}$$

Likewise for α:

$$\begin{aligned}
\frac{1}{i}\left(\frac{d\alpha}{ds}\right)_{s=0} &= \varepsilon\left(1-e^{-k_1\tau}\right) + \frac{l}{k_2}E\left(J\right)\left(1-e^{-k_2\tau}\right) \\
\frac{1}{i^2}\left(\frac{d^2\alpha}{ds^2}\right)_{s=0} &= \frac{\sigma_x^2}{2k_1}\left(1-e^{-2k_1\tau}\right) + \frac{l}{2k_2}E\left(J^2\right)\left(1-e^{-2k_2\tau}\right) \\
\frac{1}{i^3}\left(\frac{d^3\alpha}{ds^3}\right)_{s=0} &= \frac{l}{3k_2}E\left(J^3\right)\left(1-e^{-3k_2\tau}\right) \\
\frac{1}{i^4}\left(\frac{d^4\alpha}{ds^4}\right)_{s=0} &= \frac{l}{4k_2}E\left(J^4\right)\left(1-e^{-4k_2\tau}\right)
\end{aligned} \tag{23}$$

Having derived the above derivatives, and using a lengthy and tedious algebraic manipulation, the moments are given as follows:

$$m_1 = \frac{1}{i}\left[F_1 \middle| s=0 \right] = X_t e^{-k_1\tau} + Y_t e^{-k_2\tau} + \varepsilon\left(1-e^{-k_1\tau}\right) + \frac{l}{k_2}E\left(J\right)\left(1-e^{-k_2\tau}\right) \tag{24}$$

$$m_2 = \frac{1}{i^2}\left[F_2 \middle| s=0 \right] = \frac{\sigma_X^2}{2k_1}\left(1-e^{-2k_1\tau}\right) + \frac{l}{2k_2}E\left(J^2\right)\left(1-e^{-2k_2\tau}\right) + m_1^2 \tag{25}$$

$$\begin{aligned}
m_3 = \frac{1}{i^3}\left[F_3 \middle| s=0 \right] &= \frac{l}{3k_2}E\left(J^3\right)\left(1-e^{-3k_2\tau}\right) + m_1^3 \\
&+ 3m_1\left(\frac{\sigma_X^2}{2k_1}\left(1-e^{-2k_1\tau}\right) + \frac{l}{2k_2}E\left(J^2\right)\left(1-e^{-2k_2\tau}\right) \right)
\end{aligned} \tag{26}$$

$$\begin{aligned}
m_4 = \frac{1}{i^4}\left[F_4 \middle| s=0 \right] &= \frac{l}{4k_2}E\left(J^4\right)\left(1-e^{-4k_2\tau}\right) + 4m_1\left(\frac{l}{3k_2}E\left(J^3\right)\left(1-e^{-3k_2\tau}\right) \right) \\
&+ 3\left(\frac{\sigma_X^2}{2k_1}\left(1-e^{-2k_1\tau}\right) + \frac{l}{2k_2}E\left(J^2\right)\left(1-e^{-2k_2\tau}\right) \right)^2 \\
&+ 6m_1^2\left(\frac{\sigma_X^2}{2k_1}\left(1-e^{-2k_1\tau}\right) + \frac{l}{2k_2}E\left(J^2\right)\left(1-e^{-2k_2\tau}\right) \right) + m_1^4
\end{aligned} \tag{27}$$

where, assuming that the jump size distribution is normal, i.e. $N(\mu_J, \sigma_J^2)$:

$E(J)=\mu_J,\ E(J^2)=\mu_J^2+\sigma_J^2,\ E(J^3)=\mu_J^3+3\mu_J\sigma_J^2$ and $E(J^4)=\mu_J^4+6\mu_J^2\sigma_J^2+3\sigma_J^4$

Having derived the moments, one can show explicit solutions for the variance, skewness and kurtosis of the deseasonalised spike process as follows:

Variance: $m_2-m_1^2=\frac{\sigma_x^2}{2k_1}\left(1-e^{-2k_1\tau}\right)+\frac{l}{2k_2}E\left(J^2\right)\left(1-e^{-2k_2\tau}\right)$ (28)

Skewness: $\frac{E\left[\left(z-m_1\right)^3\right]}{Variance^{3/2}}=\frac{\frac{l}{3k_2}E\left(J^3\right)\left(1-e^{-3k_2\tau}\right)}{Variance^{3/2}}$ (29)

Kurtosis: $\frac{E\left[\left(z-m_1\right)^4\right]}{Variance^2}=3+\frac{\frac{l}{4k_2}E\left(J^4\right)\left(1-e^{-4k_2\tau}\right)}{Variance^2}$ (30)